The Tetrahedral Digital Waveguide Mesh

Scott A. Van Duyne
savd@ccrma.stanford.edu

Julius O. Smith III
jos@ccrma.stanford.edu

Center for Computer Research in Music and Acoustics (CCRMA)
Dept. of Music, Stanford University, Stanford, CA

Abstract

The 2D digital waveguide mesh [7, 8] has proven to be effective and efficient in the modeling of musical membranes and plates, particularly in combination with recent simplifications in modeling stiffness [6], nonlinearities [5], and felt mallet excitations [5]. The rectilinear 3D extension to the mesh had been suggested [8], and has been applied to the case of room acoustics [2]. However, it requires the use of 6-port scattering junctions, which make a multiply-free implementation impossible in the isotropic case. The 4-port scattering junctions of the 2D mesh required only an internal divide by 2, which could be implemented as a right shift in binary arithmetic. However, the 6-port junction requires a divide by 3. The multiply-free cases occur for N-port junctions in which N is a power of two [3].

We propose here a tetrahedral distribution of multiply-free 4-port scattering junctions filling space much like the molecular structure of the diamond crystal, where the placement of the scattering junctions corresponds to the placement of the carbon nuclei, and the bi-directional delay units correspond to the four tetrahedrally spaced single bonds between each pair of nuclei. We show that the tetrahedral mesh is mathematically equivalent to a finite difference scheme (FDS) which approximates the 3D lossless wave equation. We further compute the frequency- and direction-dependent plane wave propagation speed dispersion error.

1 FDS View of the Mesh

Rectilinear meshes compute an FDS approximation of the lossless wave equation [2, 8]. It is less obvious in the tetrahedral case. Figure 1 shows a small chunk of the tetrahedral mesh. We take the distance between adjacent junctions to be 1, and the junction point marked A to lie at the origin of an (x, y, z) cartesian coordinate system. We arrange the junctions $B(0, 2\sqrt{2}/3, 1/3)$, $C(\sqrt{2/3}, -\sqrt{2}/3, 1/3)$, $D(0, 0, -1)$, and $E(-\sqrt{2/3}, -\sqrt{2}/3, 1/3)$ tetrahedrally about point $A(0, 0, 0)$. The line segments between these junction points represent bi-directional delay units of the form shown in Figure 2.

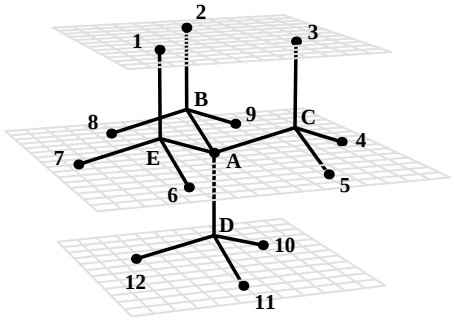

Figure 1: *3D Tetrahedral Mesh Structure*

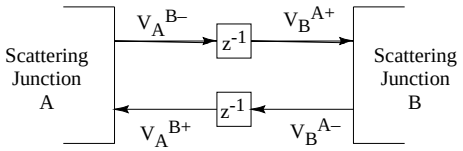

Figure 2: *Bi-Directional Delay Unit*

The equations describing the computation of the lossless 4-port scattering junctions are [3, 7, 8],

$$V_A = \frac{1}{2}\sum_{\Gamma} V_A^{\Gamma+} \quad (1)$$

$$V_A^{\Gamma-} = V_A - V_A^{\Gamma+} \quad (2)$$

where Γ ranges over the four junction points surrounding A, namely $\Gamma \in \{B, C, D, E\}$. V_A represents the junction velocity at junction A. $V_A^{\Gamma+}$ and $V_A^{\Gamma-}$ represent the input and output signals, respectively, of junction A in the direction of junction Γ.

Since the junctions are interconnected with bi-directional delay units, the input to junction A from the direction of Γ is equal to the output from Γ delayed by one sample. In the $\mathcal{Z}$-transform domain we my write this relationships as,

$$V_A^{\Gamma+} = z^{-1} V_{\Gamma}^{A-} \quad (3)$$

Using (2) and (3), we obtain an expression for the input signal to junction A from the Γ direction in terms of the junction velocities A and Γ only,

$$V_A^{\Gamma+} = z^{-1}V_\Gamma^{A-} = z^{-1}\left(V_\Gamma - V_\Gamma^{A+}\right) \quad (4)$$
$$= z^{-1}\left[V_\Gamma - z^{-1}\left(V_A - V_A^{\Gamma+}\right)\right] \quad (5)$$

which implies,

$$V_A^{\Gamma+} = \left(\frac{z^{-1}}{1-z^{-2}}\right)\left(V_\Gamma - z^{-1}V_A\right) \quad (6)$$

We substitute (6) into (1) to get an expression for the junction velocity V_A in terms of the four surrounding junction velocities V_Γ,

$$V_A = \frac{1}{2}\left(\frac{z^{-1}}{1+z^{-2}}\right)\sum_\Gamma V_\Gamma \quad (7)$$

Unfortunately, the orientations of the tetrahedra vary from point to point. Notice in Figure 1 that the tetrahedron around point A and that around point B are in *vertically opposite* orientations. However, consider the relationship between the center point A and the twelve equally spaced junctions marked 1 through 12, which are all equidistant from A, and which are *two* time steps away from A. With some imagination, one can see that the directional relationships between point A and the outer twelve points repeats itself around *every* point in the mesh, regardless of orientation of the inner four points, B, C, D, and E.

Therefore, we take note of the following relationships, which may be derived in a manner similar to (7),

$$V_\Gamma = \frac{1}{2}\left(\frac{z^{-1}}{1+z^{-2}}\right)\left(V_A + \sum_{\gamma_\Gamma} V_{\gamma_\Gamma}\right) \quad (8)$$

where $\Gamma \in \{B,C,D,E\}$ and $\gamma_B \in \{2,8,9\}$, $\gamma_C \in \{3,4,5\}$, $\gamma_D \in \{10,11,12\}$ and $\gamma_E \in \{1,6,7\}$. Plugging (8) back into (7), we get an expression for V_A in terms of the junction velocities of the twelve junctions, V_i:

$$V_A = \frac{1}{4}\left(\frac{z^{-2}}{1+z^{-2}+z^{-4}}\right)\sum_{i=1}^{12} V_i \quad (9)$$

To see that this partial difference equation approximates the continuous time wave equation, we first multiply through by the denominator in (9), inverse $\mathcal{Z}$-transform, and gather all the terms onto the left hand side. Then we view the equation as a continuous time and space expression of the form $\mathcal{F}(t,\underline{p}) = 0$, where $\mathcal{F}(t,\underline{p})$ is,

$$\sum_{k=0}^{2} v(t-2k\varepsilon,\underline{p}) - \frac{1}{4}\sum_{i=1}^{12} v(t-2\varepsilon,\underline{p}+\underline{P}_i\varepsilon) \quad (10)$$

and $\underline{p}$ is now the arbitrary spatial position of junction A, and the $\underline{P}_i$ represent the twelve directional vectors from point A to the junction points marked 1 through 12 in Figure 1, respectively. The unit time and space steps are taken to be ε.

We may expand (10) in a four dimensional Taylor series about the point $\underline{p} = (0,0,0)$ at time $t = 0$, replacing each term of (10) with something of the form,

$$\sum_{n_t}^{\infty}\sum_{n_x}^{\infty}\sum_{n_y}^{\infty}\sum_{n_z}^{\infty} \frac{v_{\underline{0}}^{(n_t,n_x,n_y,n_z)} t^{n_t} x^{n_x} y^{n_y} z^{n_z}}{n_t! n_x! n_y! n_z!} \quad (11)$$

Collecting terms and computing the limit reveals that

$$\lim_{\varepsilon\to 0}\frac{\mathcal{F}}{(2\varepsilon)^2} = u_{tt} - \frac{1}{3}\left[u_{xx} + u_{yy} + u_{zz}\right] \quad (12)$$

Evidently, the tetrahedral waveguide mesh is equivalent to an FDS approximating the continuous wave equation. The apparent wave speed is $c = \sqrt{1/3}$, which is the numerically optimal speed in the Courant-Friedrichs-Lewy sense [1, 4]. (Incidentally, we found it convenient to use the symbol manipulating feature of the mathematics processing language *Mathematica* to verify the algebra.)

2 Dispersion Analysis

To quantify dispersion error in the tetrahedral mesh, we apply a von Neumann analysis directly on the FDS [4, 7]. Essentially, we transform the FDS into the frequency domain in both time and space, replacing spatial shifts with their corresponding spatial linear phase terms. Then we observe how the spatial spectrum updates after one time sample. With this information, we can determine how fast the various plane waves travel in the mesh at each frequency. There can be no attenuation since the mesh is constructed from *lossless* scattering junctions. Therefore, the only departure from ideal behavior, aside from round-off error, is traveling-wave dispersion.

In order to avoid the difficulty of defining a discrete Fourier transform over a tetrahedrally sampled space, we consider the discrete-time/discrete-space difference scheme to be in *continuous* space by replacing the sample points in space by their corresponding generalized impulse functions, filling the regions in between them with zeros. In this formulation, the tetrahedral difference scheme applies to all points in space continuously; however, since there shall only be initial conditions at the tetrahedral mesh sampling points, the zero regions will remain at zero as the difference scheme progresses through time.

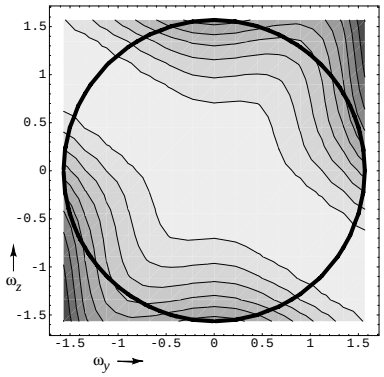

Figure 3: *Tetrahedral Dispersion:* $\omega_x = 0$

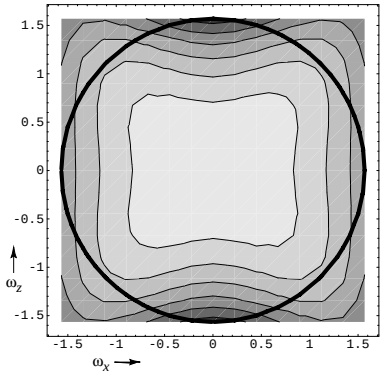

Figure 4: *Tetrahedral Dispersion:* $\omega_y = 0$

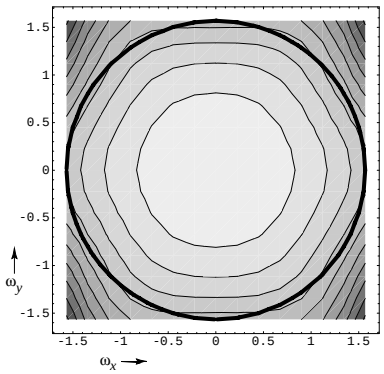

Figure 5: *Tetrahedral Dispersion:* $\omega_z = 0$

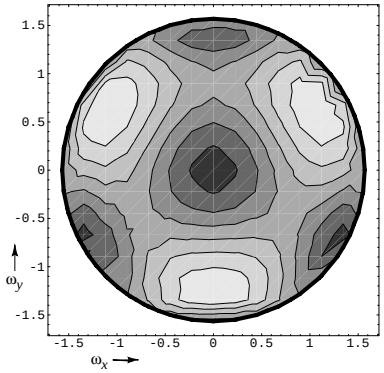

Figure 6: *Tetrahedral Dispersion:* $|\underline{\omega}| = \pi/2$

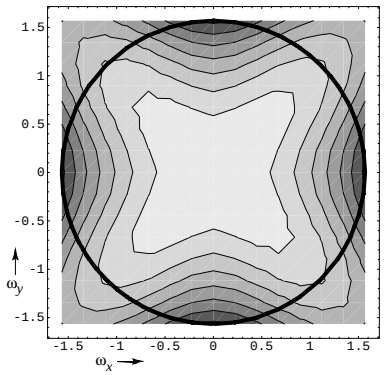

Figure 7: *Rectilinear Dispersion:* $\omega_z = 0$

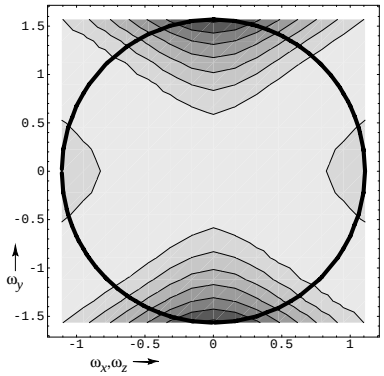

Figure 8: *Rectilinear Dispersion:* $\omega_z = \omega_x$

We may now take the spatial Fourier transform of (9) and replace the spatial positions of the twelve outer junction points with their corresponding linear phase terms, $V_i \longleftrightarrow V(\underline{\omega})e^{j\underline{P}_i^T \cdot \underline{\omega}}$, where $\underline{\omega}$ is the three-dimensional spatial frequency vector, to obtain the following quadratic expression in z^{-2}:

$$1 + bz^{-2} + z^{-4} = 0, \quad b \triangleq 1 - \frac{1}{4}\sum_{i=1}^{12} e^{j\underline{P}_i^T \cdot \underline{\omega}} \qquad (13)$$

where z^{-2} represents two time samples of delay. Due to the symmetrical orientation of vectors $\underline{P}_i$, as indicated in Figure 1, it may be shown, rather remarkably, that the value of b remains a real number be-

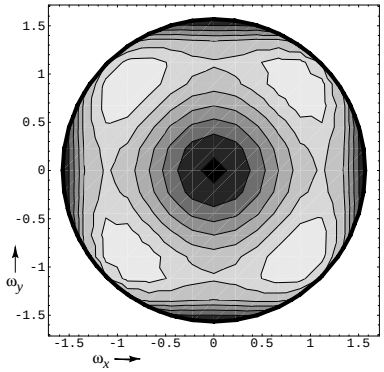

Figure 9: *Rectilinear Dispersion:* $|\underline{\omega}| = \pi/2$

tween -2 and 2 for all values of $\underline{\omega}$. Hence, we may define

$$\mathcal{G}^2(\underline{\omega}) \triangleq -\frac{b}{2} \pm j\frac{\sqrt{4-b^2}}{2} \tag{14}$$

where $\mathcal{G}$ is the *spectral amplification factor* of the spatial spectrum after *one* time sample.

It is easy to show that $|\mathcal{G}| \equiv 1$, hence plane waves propagate losslessly. We note that the phase of $\mathcal{G}$ corresponds to the spatial phase shift of a plane wave in the direction of travel in one time sample, where

$$\angle\mathcal{G} = \frac{1}{2}\arctan\frac{\pm\sqrt{4-b^2}}{b} \tag{15}$$

Hence, the *phase distance* traveled in one time sample by a spatial plane wave of frequency $|\underline{\omega}|$ and direction $\underline{\omega}$ is $c'(\underline{\omega}) = \angle\mathcal{G}/|\underline{\omega}|$, where $c'(\underline{\omega})$ is the frequency dependent speed of plane wave travel measured in space samples per time sample. (*Phase distance* corresponds to *phase advance* in time domain language.)

3 Dispersion Results

Figures 3, 4 and 5 show contour plot slices along the planes $\omega_x = 0$, $\omega_y = 0$, and $\omega_z = 0$, respectively, of the normalized plane wave speed $c'(\underline{\omega})/c$ in the tetrahedral mesh. The innermost contour line is drawn at 99% of full speed and subsequent lines are drawn at 1% intervals. Because of the spatial sampling interval, there is a Nyquist limit on the spatial frequencies which may be supported on the mesh, namely $|\underline{\omega}| < \pi$. In addition, all transfer functions definable at any one junction, and the denominators of all transfer functions definable between any pair of junctions, are functions of z^{-2}, as may be seen from Figure 2. Therefore, frequencies above $\pi/2$ are not independent, and are constrained to be a copy of the frequencies below $\pi/2$. We have superimposed a circle marking this limit in the contour plots. The central area of each plot corresponds to lower spatial frequencies, and the outer regions correspond to higher spatial frequency. The angular position of a point on each plot indicates the direction of the wave travel in the planar slice being shown. Figure 6 shows the response on the hemispherical surface, $|\underline{\omega}| = \pi/2$, where $\omega_z = \sqrt{(\pi/2)^2 - \omega_x^2 - \omega_y^2}$.

By way of comparison, we show dispersion plots for the 6-port rectilinear 3D waveguide mesh [8, 2] with the same contour line settings. We computed these following a similar procedure as that outlined above for the tetrahedral case. Figure 7 shows a horizontal slice through the origin, and Figure 8 shows a diagonal slice through $\omega_x = \omega_z$. Figure 9, again, shows the response on the hemispherical surface, $|\underline{\omega}| = \pi/2$.

Both the rectilinear and the tetrahedral mesh have reasonable dispersion characteristics. And both model a wave speed of $c = \sqrt{1/3}$ space samples per time sample. We compute that the number of tetrahedrally arranged junctions required to fill a given volume is 35% less than that required for the rectilinear mesh; and the number of bi-directional delay units required for the tetrahedral mesh is 57% less than that required for the rectilinear mesh to fill the same given volume, thus saving substantial memory. Furthermore, the tetrahedral mesh is multiply-free and may be implemented efficiently in high-speed hardware.

4 Acknowledgment

The authors are grateful to Prof. Wen-Yu Su for fruitful discussions on the topic of this paper.

References

[1] Courant, R.; Friedrichs, K. and H. Lewy. *On the Partial Difference Equations of Mathematical Physics.* United States Atomic Energy Commission, Contract No. AT(30-1)-1480. 1956.

[2] Savioja, L; Rinne, T. J. and Takala, T. "Simulation of Room Acoustics with a 3-D Finite Difference Mesh", *Proc. ICMC*, Århus, 1994.

[3] Smith, J. O. *Music Applications of Digital Waveguides.* CCRMA, Stanford Univ., Stanford, CA, Tech. Rep. STAN-M-39. 1987.

[4] Strikwerda, J. *Finite Difference Schemes and Partial Differential Equations.* Wadsworth & Brooks, Pacific Grove, CA. 1989.

[5] Van Duyne, S. A.; Pierce, J. R. and J. O. Smith. "Traveling Wave Implementation of a Lossless Mode-Coupling Filter and the Wave Digital Hammer." *Proc. ICMC*, Århus. 1994.

[6] Van Duyne, S. A. and J. O. Smith. "A Simplified Approach to Modeling Dispersion Caused by Stiffness in Strings and Plates." *Proc. ICMC*, Århus. 1994.

[7] Van Duyne, S. A. and J. O. Smith. "The 2-D Digital Waveguide Mesh." *Proc. IEEE Workshop on App. of Sig. Proc. to Audio and Acoust.*, Mohonk. 1993.

[8] Van Duyne, S. A. and J. O. Smith. "Physical Modeling with the 2-D Digital Waveguide Mesh." *Proc. ICMC*, Tokyo. 1993.